

# Research on the Application of Stewart Platform for Wave Compensation

Mingxiao Wang<sup>1</sup>, Qiang Ma<sup>2</sup> and Guoqing Sun<sup>3</sup>

<sup>1</sup>School of shipping, Shandong jiaotong University, Weihai 264200, China

<sup>2</sup>Division of Crew Education and Training Quality Management, Shandong Jiaotong University, Weihai 264200, China

<sup>3</sup>Binzhou Vocational College, Binzhou 256600, China

## Abstract

**In the field of ocean engineering, the efficiency and safety of ship operation are significantly affected by waves. Faced with the instability and safety risks of ship crane operation under complex sea conditions, a design and research method of efficient wave compensation device based on Stewart platform is proposed in this paper, aiming at developing a compensation system that can respond in real time and effectively counteract the effects of waves, so as to improve the safety and efficiency of offshore operations. Aiming at the limitation of traditional wave compensation technology, this paper adopts the BP neural network PID control algorithm combined with Stewart platform. Utilizing the Stewart platform's six-degree-of-freedom motion capability, fast compensation of wave motion is achieved. On this basis, the BP neural network PID control strategy is introduced to optimize the response speed and compensation accuracy of the system, and realize the efficient and accurate compensation of wave motion under complex sea conditions.**

## Keywords

**Stewart Platform; Neural Network; PID; Wave Compensation.**

## 1. Introduction

The working environment at sea is relatively complex, and the hull and the equipment on board are affected by various environmental factors such as their own load, weather and sea conditions, which inevitably produce various oscillatory movements on the hull [1]. The parallel Stewart mechanism has the characteristics of simple structure, strong bearing capacity and multi-scene application. Therefore, the development of Stewart platform wave compensation system is of great significance for Marine resources development and scientific research exploration.

In 1928, American James E. Gwinnett invented an entertainment device sports platform, which was the earliest application of the Stewart platform [2]. In 1949, Gough designed a tire testing equipment based on the parallel mechanical structure [3]. In 1965, British engineer Stewart published a paper on the six-degree of freedom platform, which attracted widespread attention[4]. The corresponding parallel platform was also called the Stewart platform. Stewart is also recognized as a pioneer in the field of parallel mechanisms. In the early 1870s, NASA developed a parallel mechanism platform for daily training pilots, the first time in history that a six-degree-of-freedom parallel platform was used as a flight simulation system[5].

In 1978, Australian Hunter developed a robotic arm device using a parallel mechanism[6], which is also a sign of the birth of parallel robots. At the end of the last century, through the continuous innovation of technology and the improvement of application requirements, the

development and use of parallel platforms have gradually increased. In 1994, Lewis of the United States demonstrated a VARIAX machine tool based on a parallel mechanism at an exhibition[7]. Subsequently, parallel structure machine tools have made further development, including the emergence of high-performance machine tools such as Sweden's NeosRobotics Tricept 600 machine tool[8] and Germany's Mikromat company's high-speed processing machine tools, all of which indicate that parallel machine tools have received extensive attention in modern industry. Subsequently, a company in the United States developed a 6-DOF electro-hydraulic multi-vibrator TE6-900[9]. Different from the traditional electro-hydraulic multi-vibration table, its structure optimization and control technology have been greatly improved, has been able to meet the sine signal, pulse signal and a variety of coupling instruction signal recurrence, further confirmed the superiority of the parallel mechanism. In 2005, the Fluid Transmission and Control Research Institute of Harbin Institute of Technology and the 719 Research Institute of China Shipbuilding Industry jointly developed a six-degree-of-freedom navigation simulator.

## 2. Mathematical Model of Wave Compensation Device

In order to obtain the smooth operation of Marine crane, the wave compensation system is determined by the transformation relationship between coordinate systems. The coordinate system is the reference base to describe the position attitude and motion of the ship. The determination of the space position attitude of the ship is realized according to the conversion and detection signals between the coordinate systems. In order to describe the ship's motion and derive the transformation formula of the motion coordinates, it is necessary to establish the coordinate system: the moving coordinate system on the upper platform and the fixed coordinate system on the lower platform.

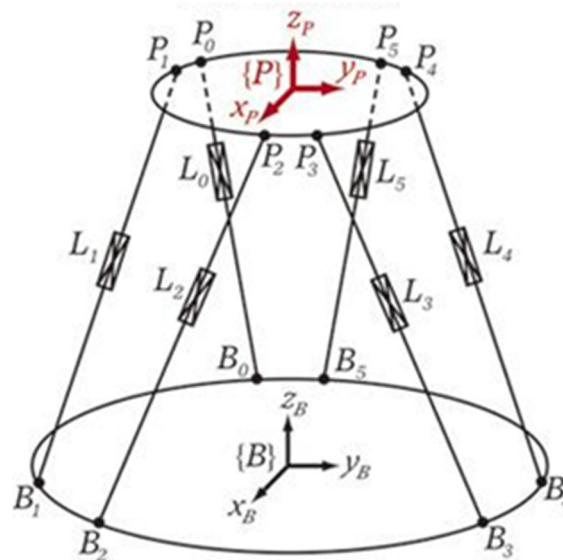
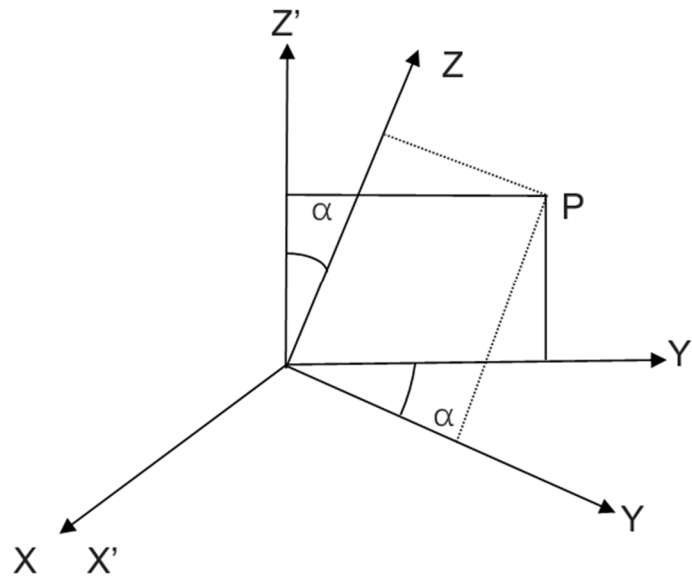


Fig 1. Stewart platform coordinate system

### 2.1. Coordinate Transformation

The purpose of the coordinate transformation is to convert the attitude change detected by the sensor into the same coordinate system to facilitate the calculation of the length of the six legs. After the ship crane operation is affected by the wave impact, there are three main degrees of freedom that have a greater impact on the crane, respectively Heave: Z-axis vertical motion, Roll: rotation around X axis, Pitch: Rotating around the Y-axis, the length of each Stewart leg is obtained by coordinate transformation, and the wave compensation for the three-degree-of-freedom motion is finally realized.

When the ship rolls, that is, the rotation Angle around the X-axis is  $\alpha$ . Taking the hinge point P of the above platform as an example, the relationship between the coordinates under the new coordinate system and the original coordinates can be obtained:



**Fig 2.** The top platform rotates around the X-axis

$$\begin{cases} X_p = X'_p \\ Y_p = Y'_p \cos \alpha - Z'_p \sin \alpha \\ Z_p = Y'_p \sin \alpha + Z'_p \cos \alpha \end{cases} \quad (1)$$

Transform the coordinates:

$$\begin{bmatrix} X_p \\ Y_p \\ Z_p \end{bmatrix} = \begin{bmatrix} 1 & 0 & 0 \\ 0 & \cos \alpha & -\sin \alpha \\ 0 & \sin \alpha & \cos \alpha \end{bmatrix} \begin{bmatrix} X'_p \\ Y'_p \\ Z'_p \end{bmatrix} \quad (2)$$

The matrix after rotation about the X-axis, or Roll, is obtained:

$$R_X(\alpha) = \begin{bmatrix} 1 & 0 & 0 \\ 0 & \cos \alpha & -\sin \alpha \\ 0 & \sin \alpha & \cos \alpha \end{bmatrix} \quad (3)$$

Similarly, the matrix of rotation  $\theta$  about the Y-axis (Pitch) can be obtained:

$$R_Y(\theta) = \begin{bmatrix} \cos \theta & 0 & \sin \theta \\ 0 & 1 & 0 \\ -\sin \theta & 0 & \cos \theta \end{bmatrix} \quad (4)$$

## 2.2. Homogeneous Transformation

The homogeneous coordinate system works by combining the traditional (n) -dimensional coordinates  $((x_1, x_2, \dots, x_n))$  extends to the (n+1) dimensional form  $((x_1, x_2, \dots, x_n, w))$ , where (w) is usually set to 1. This extension not only makes the transformation more uniform and convenient, but also allows us to represent the point at infinity, thus providing convenience for processing projection transformations. In homogeneous coordinate system, traditional geometric transformations such as translation, rotation and scaling can be accomplished by simple matrix multiplication, which improves the efficiency and accuracy of the calculation, which is difficult to achieve in non-homogeneous coordinate system. By adding an extra dimension, a homogeneous coordinate system can convert a nonlinear geometric transformation into a linear operation, making the transformation process possible through

matrix operations. This method not only simplifies the complexity of the transformation, but also improves the flexibility and efficiency of the operation.

Homogeneous transformation of the roll transformation matrix:

$$\begin{bmatrix} X_P \\ Y_P \\ Z_P \\ 1 \end{bmatrix} = \begin{bmatrix} 1 & 0 & 0 & 0 \\ 0 & \cos\alpha & -\sin\alpha & 0 \\ 0 & \sin\alpha & \cos\alpha & 0 \\ 0 & 0 & 0 & 1 \end{bmatrix} \begin{bmatrix} X'_P \\ Y'_P \\ Z'_P \\ 1 \end{bmatrix} \quad (5)$$

That is, the homogeneous transformation of the roll transformation matrix:

$$R_X = \begin{bmatrix} 1 & 0 & 0 & 0 \\ 0 & \cos\alpha & -\sin\alpha & 0 \\ 0 & \sin\alpha & \cos\alpha & 0 \\ 0 & 0 & 0 & 1 \end{bmatrix} \quad (6)$$

Similarly, the homogeneous transformation of pitching:

$$R_Y = \begin{bmatrix} \cos\theta & 0 & \sin\theta & 0 \\ 0 & 1 & 0 & 0 \\ -\sin\theta & 0 & \cos\theta & 0 \\ 0 & 0 & 0 & 1 \end{bmatrix} \quad (7)$$

Assuming the heave height is H, the homogeneous transformation is:

$$R_Z = \begin{bmatrix} 1 & 0 & 0 & 0 \\ 0 & 1 & 0 & 0 \\ 0 & 0 & 1 & H \\ 0 & 0 & 0 & 1 \end{bmatrix} \quad (8)$$

Since the crane Stewart platform is affected by both rotation and movement, the comprehensive transformation matrix is as follows:

$$R = R_Z R_Y R_X = \begin{bmatrix} 1 & 0 & 0 & 0 \\ 0 & 1 & 0 & 0 \\ 0 & 0 & 1 & H \\ 0 & 0 & 0 & 1 \end{bmatrix} \begin{bmatrix} \cos\theta & 0 & \sin\theta & 0 \\ 0 & 1 & 0 & 0 \\ -\sin\theta & 0 & \cos\theta & 0 \\ 0 & 0 & 0 & 1 \end{bmatrix} \begin{bmatrix} 1 & 0 & 0 & 0 \\ 0 & \cos\alpha & -\sin\alpha & 0 \\ 0 & \sin\alpha & \cos\alpha & 0 \\ 0 & 0 & 0 & 1 \end{bmatrix} \quad (9)$$

So:

$$R = \begin{bmatrix} \cos\theta & \sin\theta\sin\alpha & \cos\alpha\sin\theta & 0 \\ 0 & \cos\alpha & -\sin\alpha & 0 \\ -\sin\theta & \cos\theta\sin\alpha & \cos\alpha\cos\theta & H \\ 0 & 0 & 0 & 1 \end{bmatrix} \quad (10)$$

Take the length of leg  $L_0$  as an example, move the height H along the Z axis, the coordinate of point  $P_0$  is  $(X_{P_0}, Y_{P_0}, Z_{P_0})$ , the coordinate of point  $B_0$  is  $(X_{B_0}, Y_{B_0}, Z_{B_0})$ , and the homogeneous representation is:  $P_0 = [X_{P_0} \ Y_{P_0} \ Z_{P_0} \ 1]^T, B_0 = [X_{B_0} \ Y_{B_0} \ Z_{B_0} \ 1]^T$ , Combining rotation and movement gives the rotation matrix  $B_0$ :

$$B_0 = R P_0 \quad (11)$$

The coordinates after movement are calculated as follows:

$$\begin{cases} X_{B_0} = X_{P_0}\cos\theta + Y_{P_0}\sin\theta\sin\alpha + Z_{P_0}\cos\alpha\sin\theta \\ Y_{B_0} = Y_{P_0}\cos\alpha - Z_{P_0}\sin\alpha \\ Z_{B_0} = -X_{P_0}\sin\theta + Y_{P_0}\cos\theta\sin\alpha + Z_{P_0}\cos\alpha\cos\theta + H \end{cases} \quad (12)$$

The distance between the two coordinates is the length of  $L_0$ :

$$L_0 = \sqrt{(X_{P_0} - X_{B_0})^2 + (Y_{P_0} - Y_{B_0})^2 + (Z_{P_0} - Z_{B_0})^2} \quad (13)$$

### 3. BP Neural Network PID Algorithm

The architecture core of PID control system based on BP neural network [10] consists of two components. The first is the classical PID controller, which directly implements closed-loop control of the controlled object, and its three key parameters (proportion, integral, differential coefficients) are adjusted in real time through online means. Secondly, BP neural network plays the role of intelligent regulator, which intelligently adjusts the parameters of PID controller according to the real-time operating state of the system to optimize the system performance and achieve certain predetermined performance indicators.

Specifically, the output layer neurons of the BP neural network directly correspond to the three adjustable parameters of the PID controller. Through the self-learning of the network and the dynamic adjustment of the weighting coefficient, the system can gradually find the PID controller parameters matching the optimal control law, so as to achieve a more stable and efficient control effect. This kind of PID control system based on BP neural network not only improves the precision and efficiency of the control, but also enhances the adaptability and robustness of the system.

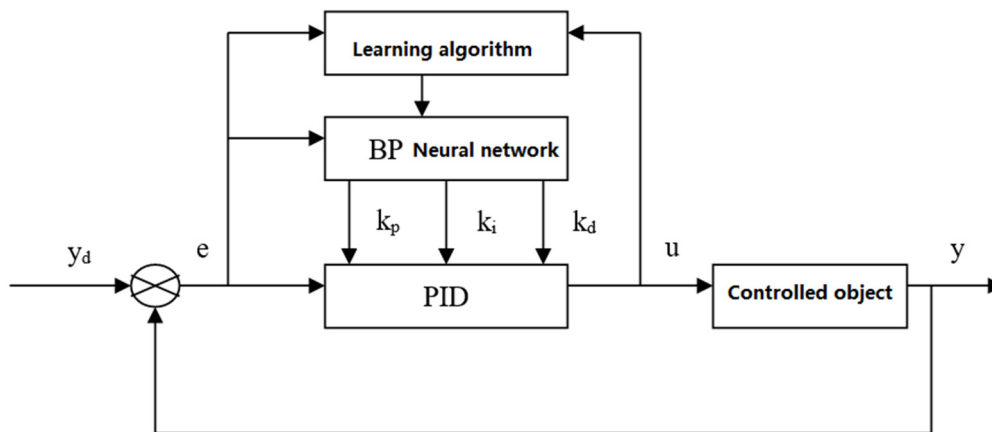


Fig 3. PID algorithm architecture of BP neural network

The expression of incremental digital PID is:

$$u(k)-u(k-1)=k_p(e(k)-e(k-1))+k_i e(k)+k_d(e(k)-2e(k-1)+e(k-2)) \tag{14}$$

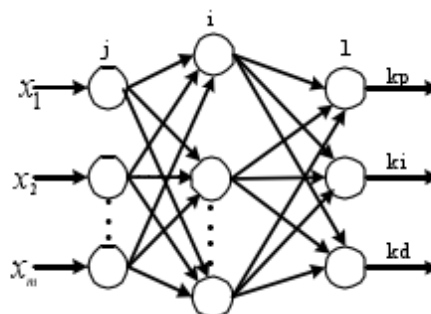


Fig 4. BP neural network framework

Where  $k_p$ ,  $k_i$  and  $k_d$  are proportional, integral and differential coefficients respectively. BP neural networks are used to train and learn the relevant nonlinear functions  $f(x)$  such as  $k_p$  (scale coefficient),  $k_i$  (integral coefficient),  $k_d$  (differential coefficient),  $u(k-1)$  (control output at the previous time) and  $e(k)$  (error at the current time) to find the best control law.

BP neural network (NN) is A three-layer structure, consisting of A input node, q implicit node and 3 output nodes. These output nodes correspond to the three parameters of the PID controller, and they must be non-negative, so the output layer neurons use the non-negative Sigmoid function as the activation function.

Based on the PID architecture of BP neural network, we can see:

$$\begin{cases} o_1^{(3)}(k)=k_p \\ o_2^{(3)}(k)=k_i \\ o_3^{(3)}(k)=k_d \end{cases} \quad (15)$$

According to the incremental PID control, it can be obtained:

$$\begin{cases} \frac{\partial u(k)}{\partial o_1^{(3)}(k)}=e(k)-e(k-1) \\ \frac{\partial u(k)}{\partial o_2^{(3)}(k)}=e(k) \\ \frac{\partial u(k)}{\partial o_3^{(3)}(k)}=e(k)-2e(k-1)+e(k-2) \end{cases} \quad (16)$$

Then the weight formula of output layer of BP neural network:

$$\Delta\omega_{li}^{(3)}(k)=\eta\delta_l^{(3)}o_i^{(2)}(k)+\gamma\Delta\omega_{li}^{(3)}(k-1) \quad (17)$$

$$\delta_l^{(3)}=e(k)\frac{\partial \hat{y}(k)}{\partial u(k)}\frac{\partial u(k)}{\partial o_l^{(3)}(k)}g'(net_l^{(3)}(k)) \quad (l=1,2,3) \quad (18)$$

Where:  $\eta$  : learning rate  $g(x)$ : output layer activation function.

Then the weight formula of the hidden layer:

$$\Delta\omega_{ij}^{(2)}(k)=\eta\delta_i^{(3)}o_j^{(2)}(k)+\gamma\Delta\omega_{ij}^{(2)}(k-1) \quad (19)$$

$$\delta_i^{(2)}=f'(net_i^{(2)}(k))\sum_{l=1}^3\delta_l^{(3)}\omega_{li}^{(3)}(k) \quad (i=1,2,3\dots q) \quad (20)$$

Where:  $f(x)$  : hidden layer activation function.

## 4. Experimental Verification of Stewart Platform

### 4.1. Experimental Platform Hardware



Fig 5. Stewart wave compensation experimental platform

The hardware components of this experiment are mainly composed of Huichuan PLC AM402, Huichuan server SV635N, up and down platform, Huichuan MS1 servo motor, electric cylinder, laser ranging sensor, electronic compass, etc.

## 4.2. Experimental Platform Software

First, the laser ranging sensor and electronic compass need to be decoded and debugged.

The laser ranging sensor supports 485 interface and MODBUS RTU communication protocol, because the Python language decoding needs to communicate with the computer, 485 to USB interface. According to the manufacturer's definition of the MODBUS RTU protocol, the send code is composed of 16-bit hexadecimal numbers: address 2 bits, function code 2 bits, start address 4 bits, register number 4 bits, check bit 4 bits, and the return code is also composed of 16-bit hexadecimal numbers: Address 2 bits, register address 2 bits, data length 4 bits, distance result 4 bits, check byte 4 bits. Where the function code 00 continuous cache, 01 single ranging, 03 continuous ranging function number read ranging data.

Electronic compass needs to be directly accessed through MODBUS communication protocol. The sending code is composed of identifier (1 byte), data length (1 byte), address code (1 byte), command word (1 byte), checksum (1 byte), and read the sending code of Pitch, Roll, and Heading from three angles: 68 04 00 04 08. The return code is composed of identifier (1 byte), data length (1 byte), address code (1 byte), command word (1 byte), data field (9 byte), checksum (1 byte), data field Pitch/Roll/Heading reading, which is a compressed BCD code. Format: SX XX YY.

The first byte S is a symbol bit, 0 represents a positive Angle, and 1 represents a negative Angle. The first byte, the second byte X, and the second byte XX are integer bits of the Angle, which are compressed BCD codes. The third byte YY is the decimal place of the Angle, which is the compressed BCD code.

The system software of the experimental platform is mainly composed of python program: 6-degree of freedom calculation program, laser ranging sensor decoding program, electronic compass decoding program, BP neural network PID algorithm, upper computer interface program, Python program and PLC communication program and Huichuan PLC program, etc., through the integration of the above programs to form a complete system software.

```
# 计算台腿的长度
legs = []
for i in range(len(xsi)):
    a = np.array([xsi[i], ysi[i], 0])
    leg_length = np.linalg.norm(b_transformed[:, i] - a)
    # 计算真实长度, 减去原始长度720mm
    deviation = leg_length - 720
    legs.append(deviation)
return legs

if __name__ == "__main__":
    try:
        while True:
            pitch, roll, heading = read_hcm365b_data()
            if pitch is not None:
                print(f"Pitch: {pitch:.2f}, Roll: {roll:.2f}, Heading: {heading:.2f}")

                # 使用读取到的角度值进行逆运动学求解
                px, py, pz = 0, 0, 780 # 设置平台顶点坐标
                XSI, YSI, XMI, YMI = [270, 270, 140, -210, -210, -140], [-50, 50, 280, 220, -220, -280], \
                    [120, 120, 15, -140, -140, 15], [-90, 90, 150, 65, -65, -150]
                roll_rad, pitch_rad, heading_rad = np.deg2rad(roll), np.deg2rad(pitch), np.deg2rad(heading)
                legs = stew_inverse(XSI, YSI, XMI, YMI, roll_rad, pitch_rad, 0, px, py, pz) # 忽略yaw影响
                print("逆运动学求解结果:", legs)
    except KeyboardInterrupt:
        # 用户中断 (如按Ctrl+C) 时退出循环
        pass
    finally:
        # 关闭串口
        ser.close()
```

Fig 6. Partial program

## 5. Conclusion

In the research of wave compensation based on Stewart platform, the BP neural network PID algorithm is introduced and successfully applied to the control strategy of wave compensation system. It not only improves the adaptive ability and control accuracy of the system, but also significantly enhances the stability and robustness of the system under complex sea conditions. Through in-depth theoretical analysis and experimental verification, it is found that the BP neural network PID algorithm can effectively learn and adapt to the dynamic characteristics of Stewart platform under the action of waves, and adjust the parameters of PID controller in real time to achieve fast and accurate compensation of wave disturbance. Compared with the traditional PID control method, this algorithm shows better performance when dealing with nonlinear, time-varying and uncertain Marine environment.

The experimental results show that the wave compensation system using BP neural network PID algorithm can be significantly reduced, and the algorithm also has a good generalization ability, and can maintain a stable compensation effect under different sea conditions, providing a reliable technical support for offshore vessels.

## References

- [1] Jun. Zhang:Simulation and experimental research of Marine simulation motion platform based on parallel mechanism [D]. Ocean University of China,2015.
- [2] Gang.Wen:Research on Control Algorithm of 6-DOF Parallel Robot [D]. Southwest Jiaotong University, 2017.
- [3] Gough V E, Whitehall S G:Universal Tyre test Machine[J]. Proc.fisita Int.tech.cong, 1962.
- [4] Stewart D. A Platform with Six Degrees of Freedom[J]. ARCHIVE Proceedings of the Institution of Mechanical Engineers 1847-1982(vols I-196), 1965, 180(1965): 371-386.
- [5] Hunt K H: Kinematic Geometry of Mechanisms. Oxford:Clarendon Press, 1978:3-9.
- [6] Ismail H, Ishak N, Tajjudin M, et al:Adaptive feedforward zero phase error tracking control with model reference for high precision X-Y table[C]. International Conference on Intelligent and Advanced Systems. IEEE, 2012.
- [7] Peng.LI: Controller Design and Application Research of high-frequency motion simulation system [D]. Harbin Institute of Technology,2013.
- [8] TENSOR TE6-900 Multi-axis, High Frequency vibration Test System[EB]. 2011.
- [9] Jinsong.Wang, Duan Guanghong, Yang Xiangdong; Research Progress of Virtual Axis Machine Tool and Discuss the successful development of VAMTIY prototype in Tsinghua University [J]. Science and Technology Review, 1998(8): 32~34.
- [10] Haifeng. Zhu, Wei.Li, Lin.Zhang:PID control based on BP neural network tuning [J]. Journal of Dynamics and Control, 2005, 3(4): 93-96.